0.7-eV GaInAs Junction for a GaInP/GaAs/GaInAs(1-eV)/GaInAs(0.7-eV) Four-Junction Solar Cell

Preprint

D.J. Friedman, J.F. Geisz, A.G. Norman,
M.W. Wanlass, and S.R. Kurtz

NOTICE

The submitted manuscript has been offered by an employee of the Midwest Research Institute (MRI), a contractor of the US Government under Contract No. DE-AC36-99GO10337. Accordingly, the US Government and MRI retain a nonexclusive royalty-free license to publish or reproduce the published form of this contribution, or allow others to do so, for US Government purposes.

This report was prepared as an account of work sponsored by an agency of the United States government. Neither the United States government nor any agency thereof, nor any of their employees, makes any warranty, express or implied, or assumes any legal liability or responsibility for the accuracy, completeness, or usefulness of any information, apparatus, product, or process disclosed, or represents that its use would not infringe privately owned rights. Reference herein to any specific commercial product, process, or service by trade name, trademark, manufacturer, or otherwise does not necessarily constitute or imply its endorsement, recommendation, or favoring by the United States government or any agency thereof. The views and opinions of authors expressed herein do not necessarily state or reflect those of the United States government or any agency thereof.

0.7-eV GaInAs JUNCTION FOR A GaInP/GaAs/GaInAs(1eV)/GaInAs(0.7eV) FOUR-JUNCTION SOLAR CELL*

D.J. Friedman, J.F. Geisz, A.G. Norman, M.W. Wanlass, and S.R. Kurtz

National Renewable Energy Laboratory, Golden, CO 80401 USA

ABSTRACT

We discuss recent developments in III-V multijunction solar cells, focusing on adding a fourth junction to the $Ga_{0.5}In_{0.5}P/GaAs/Ga_{0.75}In_{0.25}As$ inverted three-junction cell. This cell, grown inverted on GaAs so that the lattice-mismatched $Ga_{0.75}In_{0.25}As$ third junction is the last one grown, has demonstrated 38% efficiency, and 40% is likely in the near future. To achieve still further gains, a lower-bandgap $Ga_xIn_{1-x}As$ fourth junction could be added to the three-junction structure for a four-junction cell whose efficiency could exceed 45% under concentration. Here, we present the initial development of the $Ga_xIn_{1-x}As$ fourth junction. Junctions of various bandgaps ranging from 0.88 to 0.73 eV were grown, in order to study the effect of the different amounts of lattice mismatch. At a bandgap of 0.88 eV, junctions were obtained with very encouraging ~80% quantum efficiency, 57% fill factor, and 0.36 eV open-circuit voltage. The device performance degrades with decreasing bandgap (i.e., increasing lattice mismatch). We model the four-junction device efficiency vs. fourth junction bandgap to show that an 0.7-eV fourth-junction bandgap, while optimal if it could be achieved in practice, is not necessary; an 0.9-eV bandgap would still permit significant gains in multijunction cell efficiency while being easier to achieve than the lower-bandgap junction.

INTRODUCTION

The past few years have seen the introduction (sometimes reintroduction) of a variety of III-V multijunction solar cell structures with the potential for very high efficiencies. These approaches include monolithic [1-7], mechanical [8-10], and wafer-bonding schemes [11] for stacking the junctions, which may be grown lattice-matched [1-5] or lattice-mismatched [4,6,7] to their substrates. One such new device is the $Ga_{0.5}In_{0.5}P/GaAs/Ga_{0.75}In_{0.25}As$ three-junction cell [12], grown inverted so that the 1-eV $Ga_{0.75}In_{0.25}As$ junction, which is lattice-mismatched to the GaAs substrate, is grown last. This cell has demonstrated an efficiency of 37.9% at 10 suns concentration. The device that

demonstrated this efficiency had room for further optimization of current-matching and series resistance, with further incremental improvements expected to bring the efficiency above 40%. This device structure is illustrated in Fig. 1(a) as grown. A key part of the structure is the $Ga_xIn_{1-x}P$ grade, whose transparency to the light intended for the $Ga_xIn_{1-x}As$ junction is necessary for the operation of the cell. After growth of the structure, the $Ga_{0.75}In_{0.25}As$-junction back side of the structure is bonded to a foreign substrate, and the original GaAs substrate is removed.
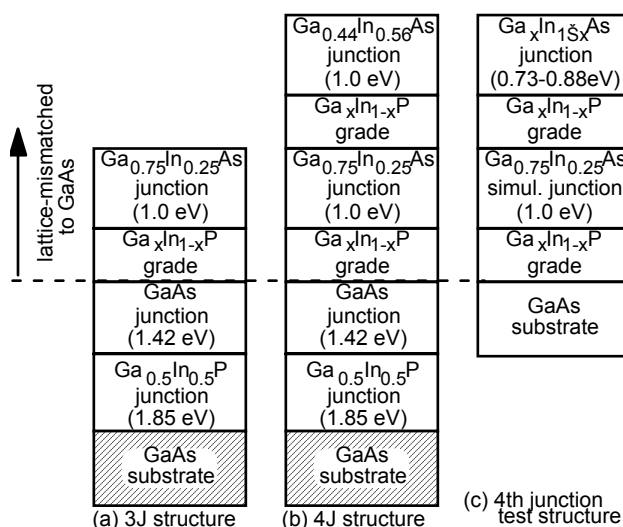

Fig. 1. Schematics of the device structures. The drawings are not to scale, and elements such as tunnel junctions and contact layers are not shown. Cross-hatching indicates substrate removed after growth. (a) Three-junction structure. (b) Proposed extension to four junctions. (c) Test structure, omitting the three higher-bandgap junctions while accounting for the mechanical effect of the $Ga_{0.75}In_{0.25}As$ third junction. As discussed below in the text, we will later consider a variant of the (a) and (b) structures in which the bandgaps of the junctions below the GaInP junction are allowed to vary.

Once this device is fully optimized, one option for further efficiency improvement in a future generation of devices based on this structure is to add a fourth junction of $Ga_xIn_{1-x}As$ with a bandgap of approximately 0.7 eV, as illustrated in Fig. 1(b). (Indeed, a very general device structure incorporating an arbitrary number of lattice-mismatched junctions has been described by Wanlass [patent pending].) At a concentration of 500 suns, such a junction would contribute an additional 5% (absolute)

efficiency for an overall real-world efficiency that could exceed 45%.

The challenge in adding an 0.7-eV fourth junction is its large lattice mismatch with the original GaAs substrate, which at 4% is twice the 2% lattice mismatch of the 1-eV third junction. It is likely that increasing lattice mismatch will be accompanied by increasing difficulty of making epilayers of the high quality required for a solar cell; note however that very good InP/GaAs cells, having the same 4% degree of mismatch, have been obtained using GaInAs grades [13]. Here, we present the initial development of the fourth junction. We study its device properties experimentally as a function of its bandgap (and therefore as a function of lattice mismatch). We also model the four-junction structure as a function of the fourth-junction bandgap, showing that high efficiencies are possible even with a fourth junction bandgap of 0.9 eV rather than 0.7 eV.

DEVICE FABRICATION

Device structures were grown by organometallic vapor-phase epitaxy. For this initial stage of development, a $Ga_xIn_{1-x}P$ grading-layer sequence including a terminating 1-µm-thick buffer layer [12], and then a 2-µm-thick 1-eV isotype $Ga_{0.75}In_{0.25}As$ layer, were first grown on a GaAs wafer. The isotype $Ga_{0.75}In_{0.25}As$ layer simulates the presence of the 1-eV third junction. Then a second $Ga_xIn_{1-x}P$ grading sequence (followed, in one case discussed below, by an $In_xAs_{1-x}P$ grade) was grown to grade from the lattice constant of the 1-eV $Ga_{0.75}In_{0.25}As$ to the lattice constant of the (nominally) 0.7-eV $Ga_xIn_{1-x}As$ junction. Finally the $Ga_xIn_{1-x}As$ junction of interest was grown, with a 2-µm-thick p-type base and an 0.1-µm n-type emitter. While the junction will eventually be used in the inverted configuration, for simplicity these test structures were grown in upright configuration. The resulting structure, shown in Fig. 1(c), accounts for the effect of the lattice-mismatched growth on the properties of the low-bandgap $Ga_xIn_{1-x}As$ junction, while bypassing the complexities of growth and measurement of the other three junctions, and the added steps of processing an inverted cell.

Junctions of various bandgaps ranging, from 0.88 to 0.73 eV, were grown in order to study the effect of the different amounts of lattice mismatch. For the lower end of the bandgap range, where it was necessary to grade to a larger lattice constant than InP, an $In_{1-x}As_xP$ grading layer was used for that final stage of the grade.

RESULTS

Figure 2 shows the internal quantum efficiencies (QE) for three variants of the device structure illustrated in Fig. 1(c). For each device, the $Ga_xIn_{1-x}P$ composition was changed by the same amount in each grade step, but different numbers of grade steps were used in the different devices. As the number of grade steps is increased, the lattice mismatch to GaAs correspondingly increases, and the bandgap of the $Ga_xIn_{1-x}As$ junction grown on the $Ga_xIn_{1-x}P$ grade structure decreases. The device with the lowest lattice mismatch, and a corresponding bandgap of 0.88 eV, has a peak QE of about 80% as shown in curve (a). The base of this device is doped to $10^{17}/cm^3$ with a corresponding depletion width of only 0.1 µm, so the high QE is due to collection of carriers by diffusion and not field-aided collection. Fitting the QE to a standard QE model yields a diffusion length longer than the base thickness of 2 µm.

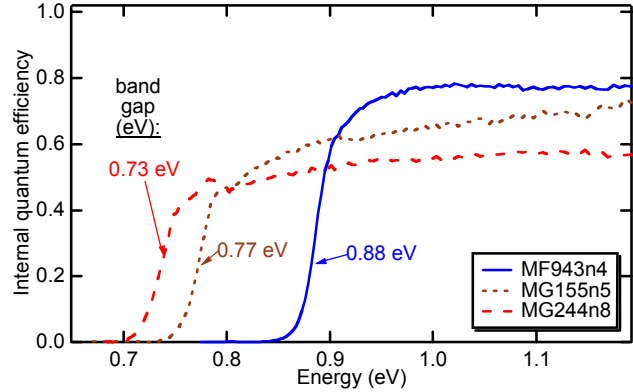Fig. 2. Quantum efficiencies for $Ga_xIn_{1-x}As$ junctions with bandgaps of (a) 0.88 eV, (b) 0.77 eV, and (c) 0.73 eV. The device IDs are indicated in the legend.

This QE, while it is less than the ~95% QE needed to obtain the full efficiency boost desired in the four-junction structure, is a promising result. However, the 0.88-eV bandgap of this device needs to be lowered in order to produce the current needed for application under the 1.85eV/1.4eV/1.0eV junctions above it. Curve (b) shows the QE for a device with more grade steps added to the graded layer, extending the grade all the way to the composition InP (i.e., $Ga_xIn_{1-x}P$ with the last step having x=0) for a resulting $Ga_{0.5}In_{0.5}As$-junction bandgap of 0.77 eV. Compared to the higher-bandgap device, the QE for the 0.77-eV device is degraded, especially in its "red" response near the band edge. The degraded red response suggests a degraded base diffusion length; fitting to the QE model yields a base diffusion length of 1 µm.

The next step in characterizing the device performance of these junctions is the measurement of the current-voltage (IV) curves under illumination. However, the choice of appropriate filtering of the incident illumination is not straightforward. We could test these devices under 1-eV lowpass filter, which would quantify their performance under the overlying 1.85eV/1.4eV/1.0-eV junctions. These conditions give the lowest J_{SC} for the device with the highest, 0.88 eV, bandgap. This tells us what we already knew, that a 0.88 eV bandgap is too high for use under a 1-eV junction. Of greater interest, we want to quantify what the performance of the devices would be if they had the desired bandgap. For this purpose, it is more meaningful to pass to the junction all of the light in the spectrum with photon energies up to about 0.3 eV above the bandgap of the junction under test, as discussed further below.

To see a full picture of the performance of these fourth junctions, we need to test them under both of these spectral filtering conditions. The most important effect of the spectral filtering on the IV curve is the light level. We therefore simulate the desired filtering conditions by computing the J_{SC} for each device from its measured QE, numerically cutting off the spectrum at a photon energy about 0.3 eV above the device's bandgap. More precisely, for a given fourth-junction bandgap, we calculate the corresponding bandgaps of the second and third junctions which would optimize the cell efficiency, as discussed below. These bandgaps are given in Table I as Opt. E_{g2} and Opt. E_{g3}, respectively. We use the E_{g3} energy as the cutoff for the numerical filter on the spectrum.

To measure the IV curve of the device, we put a GaAs filter (i.e., a 1.4-eV low-pass filter) above the device as a first approximation to the desired filtering. We then put the device into short circuit, adjust the light level to the desired light level deduced from the QE, and then measure the IV curve. The fact that the actual spectral content of the illumination differs somewhat from what it would be under the filter is not expected to change the shape of the IV curve significantly.

Table 1. Parameters characterizing the $Ga_xIn_{1-x}As$ junctions studied. V_{OC}, J_{SC}, and FF are for the IV curves of Fig. 3. For a given fourth-junction bandgap E_g and a first junction with E_g=1.85 eV, there are optimal bandgaps for the second and third junctions. These are taken from Fig. 7 and given in the table as Opt. E_{g2} and Opt. E_{g3}, respectively.

Device ID	x	E_g (eV)	V_{OC} (V)	J_{SC} (mA/cm^2)	FF (%)	Opt.E_{g2} (eV)	Opt.E_{g3} (eV)
MF943n4	0.40	0.88	0.361	10.5	57	1.56	1.21
MG155n5	0.51	0.77	0.214	9.0	48	1.51	1.15
MG244n8	0.53	0.73	0.088	8.2	30	1.48	1.12

The dark and illuminated IV curves for the devices of Fig. 1, measured as described above, are shown in Fig. 3. The device with the lowest bandgap is badly shunted, but the two higher-bandgap devices are not. The device parameters for these devices from the IV curves of Fig. 3(b) are summarized in Table I. Figure 4 shows graphically the dependence of V_{OC} on bandgap. Also shown for comparison are data points for higher-bandgap devices with near-ideal GaAs-like behavior. The V_{OC}s of the 0.88- and 0.77-eV fourth junctions fall below the line extrapolated from the GaAs-like near-ideal junctions by ~100 mV, indicating an enhanced rate of minority-carrier recombination in the junction. The 0.73-eV device has a much more significantly degraded V_{OC}. Because the difference in composition and strain between the 0.77- and 0.73-eV devices is small, the significantly degraded behavior of the 0.73-eV device suggests that the $In_{1-x}As_xP$ grade step used in this device, at its present state of development, is not of the same quality as the $Ga_xIn_{1-x}P$ grade.
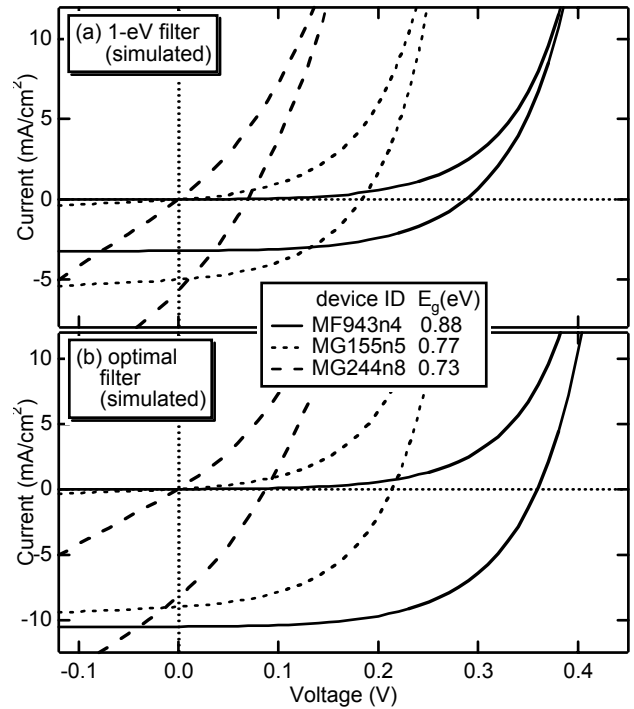

Fig. 3. IV curves for the devices whose QEs are shown in Fig. 2. As described in the text, these curves were measured illuminating the devices with as much light as would be transmitted by a low-pass filter. For panel (a) the filter was set at 1 eV; for (b) the filter was set at the value tabulated as Opt. E_{g3} in Table 1.
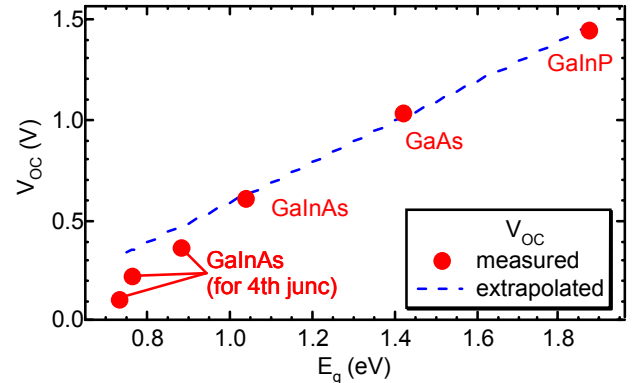

Fig. 4. V_{OC} vs. bandgap for the GaInAs fourth junctions of Table I, compared to higher-bandgap devices that are closer to ideal. The dashed line is a fit to the higher-bandgap-device data.

The composition and strain of the epilayers were studied by x-ray diffraction. Figure 5 shows the x-ray reciprocal space map for the 0.77-eV device. The compositions of the 1-eV simulated third junction and the 0.77-eV fourth-junction $Ga_xIn_{1-x}As$ layers as deduced from the reciprocal-space map are indicated, along with their strains as compared with the strain-free condition indicated by the diagonal line. These reciprocal-space maps are a powerful tool for optimizing the compositions and strain of the various mismatched layers of the structure.
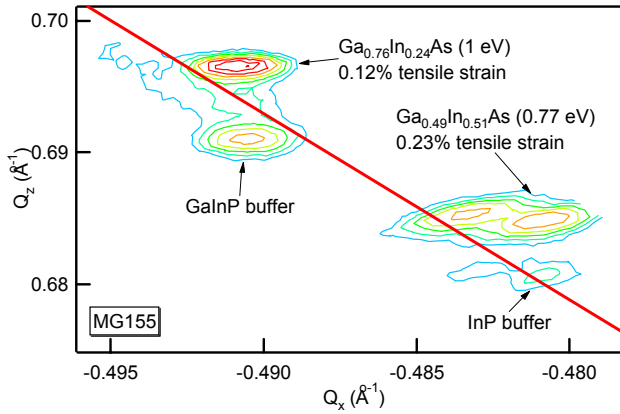
Fig. 5. X-ray reciprocal space maps for the Eg= 0.77 eV device. The compositions and strains for the $Ga_xIn_{1-x}As$ layers are indicated.

Figure 6 shows cross-sectional transmission electron microscopy (XTEM) images of the 0.88-eV GaInAs junction and the 1.0-eV GaInAs simulated junction for device MF943. The images show that the dislocations are largely confined to the GaInP grading layers. In these particular images, no dislocations are seen in the GaInAs layers, due to the extremely high magnification of the images compared to the threading dislocation density.
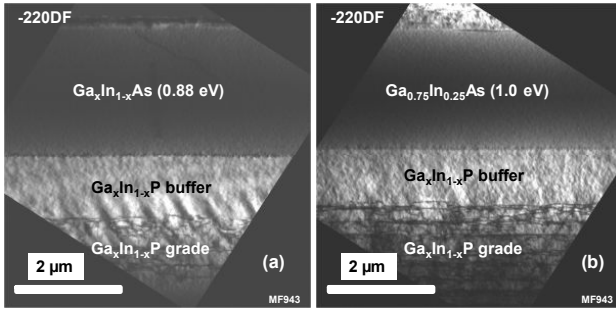

Fig. 6. XTEM images of (a) the 0.88-eV junction and (b) the 1.0-eV simulated junction for device MF943.

DISCUSSION

The next steps in the development of this lattice-mismatched fourth junction will involve manipulation of the grading layer to improve the device performance by minimizing strain-generated structural defects. Such manipulation could include the number of steps used in the grade, but could also involve moving from $Ga_xIn_{1-x}P$ to alternative alloys for the grade material.

Because the device data shown here indicate that it is increasingly difficult to get good device quality in the fourth junction with decreasing bandgap, it is worth asking whether a 0.7-eV bandgap is really necessary, or if a higher bandgap might suffice. A 0.7-eV fourth junction is called for if the bandgaps of the top three junctions are fixed at 1.85/1.42/1.0 eV. However, in practice it is possible to have the second-junction bandgap be higher than 1.42 eV while maintaining the desired lattice-matching to GaAs, by going to a GaInAsP composition. Likewise, the bandgap of the lattice-mismatched GaInAs

third junction could easily be raised simply by not grading the lattice constant so far from that of GaAs.Ideally, the top-junction bandgap should also be raised, but this has proven challenging (although see [14]). For this reason and for simplicity, we compute for idealized junctions the optimal second- and third-junction bandgaps as a function of the fourth-junction bandgap, for a top-junction bandgap fixed at 1.85 eV. The junctions are optically thinned as necessary. The resulting optimal second- and third-junction bandgaps, and the corresponding four-junction device efficiency, are shown in Fig. 7 for illumination conditions of 500 suns under the low-AOD spectrum.
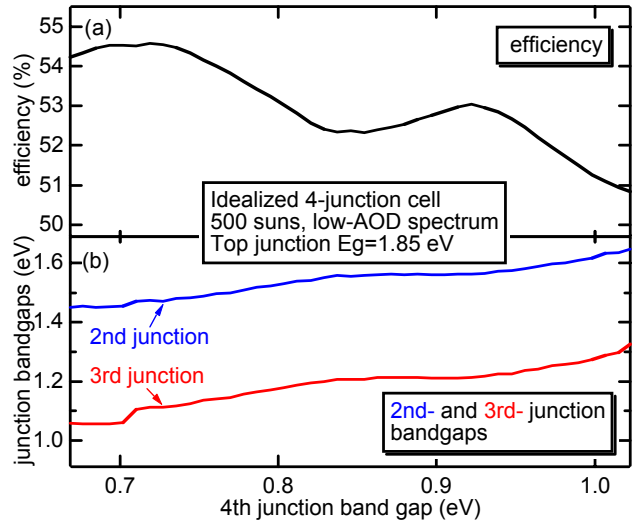

Fig. 7. (a) Four-junction device efficiency at 500 suns concentration, and (b) the corresponding optimal 2nd and 3rd junction bandgaps, for an idealized four-junction device with top-junction bandgap fixed at 1.85 eV. A finite reflectivity representative of a two-layer antireflective coat is assumed.

The figure shows that raising the fourth-junction bandgap from 0.7 eV to 0.93 eV, while adjusting the second and third junction bandgaps to 1.56 and 1.21 eV respectively, results in an efficiency loss of only 1.5%. The reason for this is that there is very little light in the terrestrial spectrum between 0.8 and 0.9 eV due an to atmospheric absorption band that removes most of the light in that spectral range. Calculating the efficiency of the 1.85/1.42/1.0-eV three-junction device in the same manner as for Fig. 7 gives an efficiency of 49%. Thus, there is 4% (absolute) efficiency to be gained by going from the three-junction to the four-junction structure with a fourth-junction bandgap of 0.9 eV, but only an additional 1.5% (absolute) may be further gained by going to a fourth-junction bandgap of 0.7 eV.

These calculations, motivated by the relative ease in fabricating a high-quality 0.9-eV junction compared to an 0.7-eV junction, suggest that in practice the former may be the preferred realization of the four-junction structure. Furthermore, 0.9-eV GaInAs is much less mismatched to GaAs (mismatch $\Delta a/a_0$=2.8%) than is 0.7-eV GaInAs (mismatch $\Delta a/a_0$=3.9%). The larger lattice mismatch of the 0.7-eV GaInAs would require a thicker grading layer, which would require more time to grow. The larger lattice

mismatch would also increase the difficulty of mitigating bowing of the wafer due to residual strain in the epilayer.

As an alternative to the four-junction structure, one may reexamine the three-junction structure, now considering the second- and third-junction bandgaps to be variable. As in the calculation in Fig. 7, we calculate the efficiency of this structure as a function of the third (bottom) junction bandgap, optimizing the second-junction bandgap while keeping the top junction fixed at 1.85 eV. The resulting efficiency and optimal second-junction bandgap are shown in Fig. 8. The results may be directly compared to Fig. 7, and for convenience the four-junction efficiency from Fig. 7 is shown in Fig. 8 as the dashed curve. The crosses on the efficiency and bandgap curves in Fig. 8 shows the 1.85/1.42/1.0-eV configuration. The figure shows that if the second-junction bandgap is lowered slightly to 1.34 eV, the efficiency increases by almost 2%. This is only half the efficiency gained by going to the four-junction structure with a 0.9-eV fourth junction; the total amount of lattice mismatch is no less; and the second junction would no longer be lattice-matched to GaAs. However, the three-junction structure is simpler and would require one less tunnel junction, so it may well be worth considering as an alternative or an intermediate step to the four-junction structure.
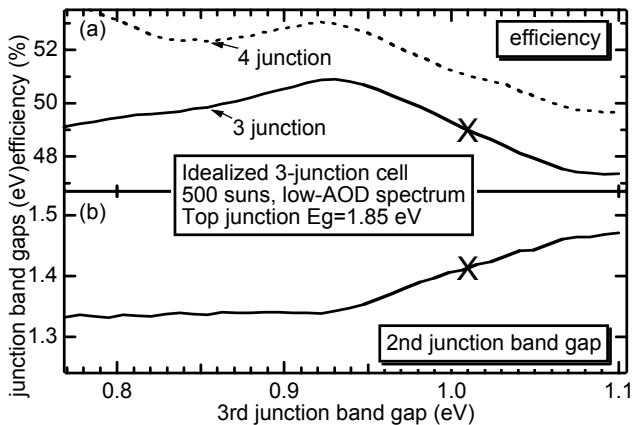

Fig. 8. (a) Three-junction device efficiency at 500 suns concentration, and (b) the corresponding optimal second junction bandgap, for an idealized three-junction device with top junction bandgap fixed at 1.85 eV. A finite reflectivity representative of a two-layer AR coat is assumed. Also shown for comparison in (a) as the dashed curve is the four-junction efficiency from Fig. 7 (a). The crosses mark the 1.85/1.42/1.0-eV configuration.

CONCLUSIONS

We have grown $Ga_xIn_{1-x}As$ junctions with bandgaps from 0.88 to 0.73 eV lattice-mismatched to GaAs, intended for use as the bottom junction of the four-junction extension of the GaInP/GaAs/ $Ga_xIn_{1-x}As$ inverted solar cell. The 0.88-eV junction showed a QE of 80% without the use of field-aided carrier collection, a promising initial result. Making high-quality junctions becomes increasingly challenging with decreasing bandgap, suggesting that 1.85/1.56/1.21/0.93 eV may be the preferred bandgap configuration. Real-world efficiency for such a device is projected to be near 45% under concentration.

REFERENCES

[1] R.R. King et al., "Pathways to 40%-efficient concentrator photovoltaics", *20th European Photovoltaic Solar Energy Conference*, 2005, pp. 118-123.
[2] M. Meusel et al., "European roadmap for the development of III-V multi-junction space solar cells", *19th European Photovoltaic Solar Energy Conference*, 2004, pp. 3581-3586.
[3] M.W. Wanlass et al., "Advanced high-efficiency concentrator tandem solar cells", *22nd IEEE Photovoltaic Specialists Conference*, 1991, pp. 38-45.
[4] M.A. Stan et al., "InGaP/InGaAs/Ge High Concentration Solar Cell Development at Emcore", *31st IEEE Photovoltaic Specialists Conference*, 2005, pp. 770-773.
[5] A.J. Ptak, D.J. Friedman, S. Kurtz, and J. Kiehl, "Enhanced-depletion-width GaInNAs solar cells grown by molecular-beam epitaxy", *Proceedings of the 31st IEEE Photovoltaic Specialists Conference*, 2005, pp. 603-606.
[6] R.R. King et al., "Metamorphic GaInP/GaInAs/Ge Solar Cells", *28th IEEE Photovoltaic Specialists Conference*, 2000, pp. 982.
[7] F. Dimroth et al., "Metamorphic $Ga_yIn_{1-y}P/Ga_{1-x}In_xAs$ tandem solar cells for space and for terrestrial concentrator applications at C>1000 suns", *Prog. Photovolt. 9*, 2001, pp. 165-178.
[8] L.M. Fraas et al., "Over 35% Efficient GaAs/GaSb Stacked Concentrator Cell Assemblies for Terrestrial Applications", *21st IEEE Photovoltaic Specialists Conference*, 1990, pp. 190-195.
[9] L. Fraas et al., "Over 30% Efficient InGaP/GaAs/GaSb Cell-Interconnected-Circuits for Line-Focus Concentrator Arrays", *28th IEEE Photovoltaic Specialists Conference*, 2000, pp. 1150.
[10] A.W. Bett et al., "Development of III-V-Based Concentrator Solar Cells and their Applications in PV-Modules", *29th IEEE Photovoltaic Specialists Conference*, 2002, pp. 844-847.
[11] J.M. Zahler et al., "Wafer-Bonding and Layer Transfer Processes for-Junction High Efficiency Solar Cells", *29th IEEE Photovoltaic Specialists Conference*, 2002, pp. 1039-1042.
[12] M.W. Wanlass et al., "Lattice-Mismatched Approaches for High Performance III-V Photovoltaic Energy Converters", *Proceedings of the 31st IEEE Photovoltaic Specialists Conference*, 2005, pp. 530-535.
[13] M.W. Wanlass et al., "High-Efficiency, Thin-Film InP Concentrator Solar Cells", *J Electron Mater 20*, 1991, pp. 1019-1024.
[14] J.M. Olson et al, "Effect Of Sb On The Properties Of GaInP Top Cells", *this proceedings*.